Applied Catalysis B: Environmental 119–120 (2012) 117–122

Contents lists available at SciVerse ScienceDirect

Applied Catalysis B: Environmental

journal homepage: www.elsevier.com/locate/apcatb

Identification of active sites for CO and CH_4 oxidation over $PdO/Ce_{1-x}Pd_xO_{2-\delta}$ catalysts

Lian Meng[a], Jian-Jun Lin[a], Zhi-Ying Pu[b], Liang-Feng Luo[c], Ai-Ping Jia[a], Wei-Xin Huang[c], Meng-Fei Luo[a,*], Ji-Qing Lu[a,**]

[a] Zhejiang Key Laboratory for Reactive Chemistry on Solid Surface, Institute of Physical Chemistry, Zhejiang Normal University, Jinhua 321004, China
[b] Research Center of Analysis and Measurement, Zhejiang University of Technology, Hangzhou 310014, China
[c] Hefei National Laboratory for Physical Sciences at the Microscale and Department of Chemical Physics, University of science and Technology of China, Hefei 230026, China

ARTICLE INFO

Article history:
Received 21 December 2011
Received in revised form 21 February 2012
Accepted 28 February 2012
Available online 7 March 2012

Keywords:
PdO_x species
$Ce_{1-x}Pd_xO_{2-\delta}$ solid solution
Active site
Specific reaction rate
Acid treatment

ABSTRACT

A $PdO/Ce_{1-x}Pd_xO_{2-\delta}$ catalyst containing surface PdO_x (x = 1–2) species and $Ce_{1-x}Pd_xO_{2-\delta}$ solid solution was prepared by a solution combustion method. It was found that the surface PdO_x species could be removed by nitric acid treatment. Also, partial Pd^{4+} cations in the CeO_2 lattice migrated to the surface to form surface PdO_x species after high temperature calcination (500 °C). The catalyst was tested for catalytic CO and CH_4 oxidation. For CO oxidation, the specific reaction rate of the surface PdO_x species (673.4 $\mu mol_{CO}\ g_{Pd}^{-1}\ s^{-1}$) was 249 times as high as that of the $Ce_{1-x}Pd_xO_{2-\delta}$ solid solution (2.7 $\mu mol_{CO}\ g_{Pd}^{-1}\ s^{-1}$), due to the fact that the surface PdO_x species provided CO chemisorption sites. While for CH_4 oxidation, the specific reaction rate of the $Ce_{1-x}Pd_xO_{2-\delta}$ solid solution (7.5 $\mu mol_{CH_4}\ g_{Pd}^{-1}\ s^{-1}$) was higher than that of the $PdO/Ce_{1-x}Pd_xO_{2-\delta}$ catalyst (2.8 $\mu mol_{CH_4}\ g_{Pd}^{-1}\ s^{-1}$), due to the covered $Ce_{1-x}Pd_xO_{2-\delta}$ surface by surface PdO_x species.

1. Introduction

The catalytic oxidation of CO and hydrocarbons are key reactions in many industrial chemical processes, as well as pollution control for automotives and industrial processes [1]. Particularly, catalytic total oxidation of methane is an effective way to use methane as an environment-friendly fuel [2]. PdO catalysts supported on oxide carriers are very active for the oxidation of CH_4 and CO. In particular, PdO/CeO_2 catalyst has attracted much attention due to its high activity which results from the unique redox property of CeO_2 [3,4] and the strong interaction between PdO and CeO_2 [5,6]. The catalytic behaviors of PdO/CeO_2 catalysts strongly depend on the preparation conditions, by which different Pd species may present in the catalyst. For example, Pd species may be in forms of Pd particles [7,8], PdO_x (x = 1–2) species [9,10] and $Ce_{1-x}Pd_xO_{2-\delta}$ solid solution formed by strong interactions between Pd and the ceria support [11]. The complexity of Pd species in $PdO–CeO_2$ thus makes it difficult to identify the active sites/phase for the oxidation reaction. It is believed that PdO_x species are the active sites for CO and CH_4 oxidation [12–15]. However, whether the surface PdO_x species or the Pd^{n+} (n = 2–4) cations in form of $Ce_{1-x}Pd_xO_{2-\delta}$ solid solution contribute to the activity is still in debate. Luo et al. [13] reported that surface PdO species were the active sites for the two reactions, while Colussi et al. [16] concluded that Pd^{2+} in $Ce_{1-x}Pd_xO_{2-\delta}$ solid solution promotes CH_4 oxidation activity. Thus, it can be seen that in order to clarify the active sites/phase, well designed catalysts with each PdO_x species separately existing in the catalyst are required. Very recently, we [17] identified different PdO species in $PdO–CeO_2$ catalysts, and their contributions to CO oxidation were also quantitatively evaluated. For CH_4 oxidation, Mayernick et al. [15,18] carried out DFT calculation and found that the methane activation barrier over the $Ce_{1-x}Pd_xO_{2-\delta}$ surface is lower than that over PdO surfaces, which is due to the enhanced reducibility of CeO_2 surface by the incorporation of Pd ions into the CeO_2 lattice.Therefore, to experimentally distinguish the catalytic behaviors of surface PdO_x species and Pd species in CeO_2 lattice for CO and CH_4 oxidation are of interest. Furthermore, note that CH_4 oxidation usually occurs at high temperature, stability of the $PdO–CeO_2$ catalyst must be concerned. In this work, several $PdO–CeO_2$ catalysts were prepared and transformation of Pd species under high temperature calcination was studied. These catalysts were tested for CH_4 oxidation, as well as CO oxidation to illustrate the different roles of the Pd species in these two reactions. The contributions of each Pd species to the reaction were also evaluated.

* Corresponding author. Tel.: +86 579 82283910; fax: +86 579 82282595.
** Corresponding author. Fax: +86 579 82282595.
E-mail addresses: mengfeiluo@zjnu.cn (M.-F. Luo), jiqinglu@zjnu.cn (J.-Q. Lu).

0926-3373/$ – see front matter © 2012 Elsevier B.V. All rights reserved.
doi:10.1016/j.apcatb.2012.02.036

2. Experimental

2.1. Catalyst preparation

A $PdO/Ce_{1-x}Pd_xO_{2-\delta}$ catalyst was prepared by a solution-combustion method [19]. The detailed process was as follows: 25.04 g of $(NH_4)_2Ce(NO_3)_6$ (45.61 mmol, 99.0%) was dissolved in 16 ml of deionized water in a porcelain crucible with 100 ml capacity. $Pd(NO_3)_2$ (0.93 mmol, 99.0%) aqueous solution and $C_2H_5NO_2$ (120.63 mmol, 99.0%) were added to the Ce-containing solution. The mixture contained $(NH_4)_2Ce(NO_3)_6$, $Pd(NO_3)_2$ and $C_2H_5NO_2$ with a molar ration of 0.98:0.02:2.59. Then, the porcelain crucible was introduced into a muffle furnace maintained at 350 °C. Initially the solution boiled with frothing, foaming and ignited to burn with a flame yielding a solid product. The solid was calcined at 800 °C in air for 4 h, and the resulting sample was denoted as $PdO/Ce_{1-x}Pd_xO_{2-\delta}$.

A $Ce_{1-x}Pd_xO_{2-\delta}$ catalyst was obtained by treating the $PdO/Ce_{1-x}Pd_xO_{2-\delta}$ with nitric acid. 1 g of the $PdO/Ce_{1-x}Pd_xO_{2-\delta}$ catalyst was immersed in a heat concentrated nitric acid (15 ml, 50 vol.%) for 1 h then filtered. The above process was repeated for three times. Finally, the obtained solid was washed with plenty of deionized water to remove the residual nitric acid and dried at 90 °C overnight. The dried sample was characterized by Fourier transform infrared spectroscopy (FTIR) to confirm that there was no residual NO_3^- in the sample. The sample was denoted as $Ce_{1-x}Pd_xO_{2-\delta}$.

A post treated $Ce_{1-x}Pd_xO_{2-\delta}$ catalyst was obtained by calcining the $Ce_{1-x}Pd_xO_{2-\delta}$ catalyst at 500 °C in air for 4 h, and denoted as $Ce_{1-x}Pd_xO_{2-\delta}$-C.

A PdO/CeO_2 catalyst with a Pd loading of 1.70 wt.% was obtained by a conventional impregnation method. The CeO_2 support was prepared in a similar manner as the $PdO/Ce_{1-x}Pd_xO_{2-\delta}$ catalyst and calcined in air at 800 °C for 4 h. The obtained CeO_2 was immersed in aqueous solution of $Pd(NO_3)_2$ for 24 h. The mixture was dried at 90 °C under stirring, and then the solid was dried at 120 °C overnight, followed by calcination at 400 °C for 4 h in air.

2.2. Characterizations

X-ray diffraction (XRD) patterns were collected on a PANalytical X'Pert PRO MPD powder diffractometer using Cu Kα radiation (λ = 0.1542 nm). The working voltage was 40 kV and the working current was 40 mA. The patterns were collected in a 2θ range from 10° to 110°. The lattice parameter and the mean crystallite size were determined by the Rietveld method using JADE 6.5 software.

Elemental compositions of the catalysts were determined by X-ray fluorescence (XRF) analysis, on an ARL ADVANT'X Intelli Power 4200 scanning X-ray fluorescence spectrometer. The results were analyzed using UniQuant non-standard sample quantitative analysis software.

Transmission electron microscopy (TEM) investigations were carried out using a JEM-2100F field emission electron microscope operated at 200 kV.

X-ray photoelectron spectroscopy (XPS) data were obtained on an ESCALab 250 electron spectrometer from Thermo Scientific Corporation with monochromatic 150 W AlKα radiation. Pass energy for the narrow scan is 30 eV. The base pressure was about 6.5×10^{-10} mbar. The binding energies were referenced to the C1s line at 284.6 eV from contaminant carbon.

Diffuse reflectance infrared Fourier transform (DRIFT) spectra of the samples were recorded using a Nicolet 6700 spectrometer equipped with a MCT detector and a diffuse reflectance cell (Harrick CHC-CHA-3), with a resolution of 4 cm^{-1}. An accumulation of 32 scans was used for collecting the spectra. About 20 mg of the catalyst was placed in the cell and pretreated at 300 °C for 1 h in a flow of Ar (30 ml min^{-1}) in order to remove water and carbonate in the catalyst. Subsequently, the system was cooled down to 30 °C and the background spectrum was recorded. After the introduction of the gas mixture (1 vol.% CO in Ar, 30 ml min^{-1}) for 30 min, the catalyst was purged with Ar for 30 min to remove the gaseous and physisorbed CO, and then a spectrum was collected.

Table 1
Cell parameters and crystallite sizes of $PdO/Ce_{1-x}Pd_xO_{2-\delta}$, $Ce_{1-x}Pd_xO_{2-\delta}$, $Ce_{1-x}Pd_xO_{2-\delta}$-C, PdO/CeO_2 and CeO_2 catalysts.

Sample	Pd content (wt.%)		Cell parameters (nm)	Crystal. size of CeO_2 (nm)
	Total	Surface		
$PdO/Ce_{1-x}Pd_xO_{2-\delta}$	1.70	0.20	0.5406	18.7
$Ce_{1-x}Pd_xO_{2-\delta}$	1.50	0	0.5407	18.3
$Ce_{1-x}Pd_xO_{2-\delta}$-C	1.50	0	0.5409	18.5
PdO/CeO_2	1.68	1.68	0.5411	37.6
CeO_2	0	0	0.5411	33.7

2.3. Catalytic testing

The reaction was carried out in a quartz tubular (i.d. = 6 mm) fixed-bed reactor under atmospheric pressure. 200 mg of the catalyst (80–100 mesh) was loaded in the reactor and the reaction temperature was monitored by a thermocouple placed in the middle of the catalyst bed. The total flow rate was 40 ml min^{-1}, corresponding to a space velocity of 12,000 ml g_{cat}^{-1} h^{-1}. The catalyst was directly exposed to the reaction without any pretreatment. For CO oxidation, a mixture of 0.95 vol.% CO and 1.75 vol.% O_2 balanced by N_2 was introduced as the reactants. Every temperature was stabilized for 30 min before analysis. The CO concentration in the reactor effluent was analyzed using an Agilent 6850 gas chromatograph equipped with a TCD detector and an HP PLOT (30 m × 0.32 mm × 12 μm) column. For CH_4 oxidation, the reactants contain a mixture of 0.5 vol.% CH_4, 3 vol.% O_2 and 96.5 vol.% N_2. The CH_4 concentration was analyzed using a Shimadzu GC-14 gas chromatograph equipped with a FID detector and a Supelcowax-10 (30 m × 0.25 mm × 0.25 μm) column.

Conversion of CO and CH_4 was calculated as follows:

$$\text{Conversion}\ (\%) = \frac{C_{in} - C_{out}}{C_{in}} \times 100 \quad (1)$$

C_{in} and C_{out} were the CO and CH_4 concentrations in the feed gas and products, respectively.

Specific reaction rate of the prepared catalyst based on per unit of Pd was calculated as follows:

$$\text{Specific reaction rate} = \frac{F \times X}{m_{Cat} \times X_{Pd}} \quad (2)$$

where F is the flow rate of CO or CH_4 in μmol s^{-1}, X is the CO or CH_4 conversion at 130 °C or 350 °C, m_{Cat} is the catalyst weight (g), X_{Pd} is the Pd content in the catalyst (shown in Table 1).

For the specific reaction rate of the surface PdO_x of the $PdO/Ce_{1-x}Pd_xO_{2-\delta}$ at CO oxidation, it was defined as follows:

$$\text{Specific reaction rate} = \frac{A_1 \times B_1 - A_2 \times B_2}{\Delta X_{Pd}} \quad (3)$$

where A_1 and A_2 are the specific reaction rates of $PdO/Ce_{1-x}Pd_xO_{2-\delta}$ and $Ce_{1-x}Pd_xO_{2-\delta}$ catalyst for CO oxidation, respectively. B_1 and B_2 are the Pd contents of these catalysts. ΔX_{Pd} is the surface Pd content on the surface of catalyst, calculated by the difference of Pd contents between the $PdO/Ce_{1-x}Pd_xO_{2-\delta}$ and $Ce_{1-x}Pd_xO_{2-\delta}$ catalysts.

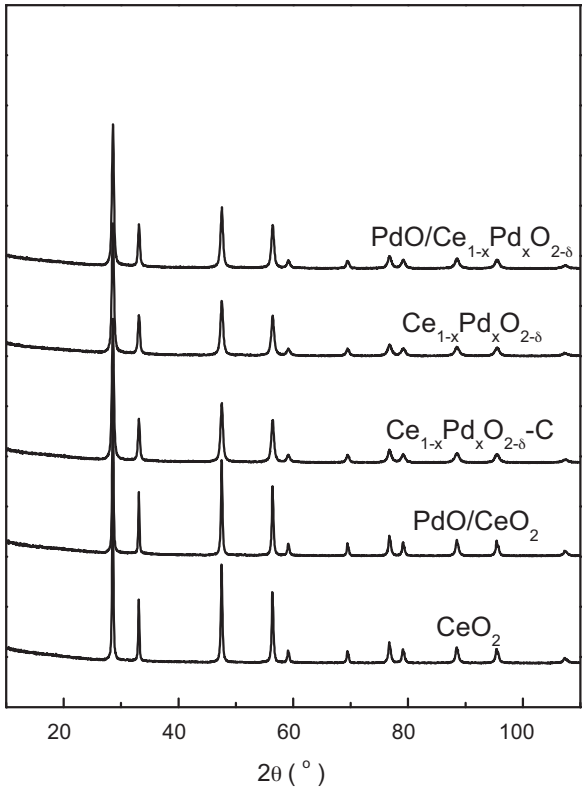

Fig. 1. XRD patterns of PdO/$Ce_{1-x}Pd_xO_{2-\delta}$, $Ce_{1-x}Pd_xO_{2-\delta}$, $Ce_{1-x}Pd_xO_{2-\delta}$-C, PdO/CeO_2 and CeO_2 catalysts.

3. Results and discussion

3.1. Structural characterization

Fig. 1 shows the XRD patterns of the PdO/$Ce_{1-x}Pd_xO_{2-\delta}$, $Ce_{1-x}Pd_xO_{2-\delta}$, $Ce_{1-x}Pd_xO_{2-\delta}$-C, PdO/CeO_2 and CeO_2 catalysts. It is found that no diffraction peaks due to PdO or Pd phase and only diffraction peaks due to the cubic CeO_2 phase are observed, implying that the Pd species may be highly dispersed on the catalyst surface or in the lattice of CeO_2.

Table 1 lists cell parameters and crystallite sizes of the PdO/$Ce_{1-x}Pd_xO_{2-\delta}$, $Ce_{1-x}Pd_xO_{2-\delta}$, $Ce_{1-x}Pd_xO_{2-\delta}$-C, PdO/CeO_2 and CeO_2 catalysts. It can be seen that the PdO/$Ce_{1-x}Pd_xO_{2-\delta}$ catalyst has a Pd content of 1.70 wt.%. After the nitric acid treating PdO/$Ce_{1-x}Pd_xO_{2-\delta}$, namely, the $Ce_{1-x}Pd_xO_{2-\delta}$ has a Pd content of 1.50 wt.%, suggesting that by using the solution combustion method, most of the Pd species penetrate into the CeO_2 lattice and less Pd species exist on the $Ce_{1-x}Pd_xO_{2-\delta}$ surface. Thus, in the PdO/$Ce_{1-x}Pd_xO_{2-\delta}$ or $Ce_{1-x}Pd_xO_{2-\delta}$ catalyst, the value of x is about 0.024. It is also found that the PdO/$Ce_{1-x}Pd_xO_{2-\delta}$ and $Ce_{1-x}Pd_xO_{2-\delta}$ catalysts have similar cell parameters and crystallite sizes, indicating that the nitric acid treatment hardly changes the structure of the $Ce_{1-x}Pd_xO_{2-\delta}$ solid solution. However, the lattice parameters of the PdO/$Ce_{1-x}Pd_xO_{2-\delta}$ and $Ce_{1-x}Pd_xO_{2-\delta}$ catalysts are lower than that of the pure CeO_2. This is because the radius of Pd^{2+} ion (0.84 Å) or Pd^{4+} ion (0.62 Å) is smaller than that of Ce^{4+} (0.99 Å), leading to a decline in lattice parameter when Ce^{4+} ions are partially substituted by Pd^{2+} or Pd^{4+} ions to form a $Ce_{1-x}Pd_xO_{2-\delta}$ solid solution [19]. Meanwhile, the formation of $Ce_{1-x}Pd_xO_{2-\delta}$ solid solution inhibits the growth of crystallite as the crystallite size of the PdO/$Ce_{1-x}Pd_xO_{2-\delta}$ or $Ce_{1-x}Pd_xO_{2-\delta}$ catalyst (about 18 nm) is smaller than that of the pure CeO_2 (33.7 nm). In comparison, the cell parameter of $Ce_{1-x}Pd_xO_{2-\delta}$-C is slightly larger than those of the PdO/$Ce_{1-x}Pd_xO_{2-\delta}$ and $Ce_{1-x}Pd_xO_{2-\delta}$ catalysts, but smaller than pure CeO_2. This implies that when the acid treated sample is calcined at 500 °C, some Pd species in the $Ce_{1-x}Pd_xO_{2-\delta}$ solid solution migrate to the surface and consequently form surface PdO_x species. Table 1 also shows that the PdO/CeO_2 catalyst has the same cell parameters with pure CeO_2, demonstrating that there is no $Ce_{1-x}Pd_xO_{2-\delta}$ solid solution formed and PdO species wholly exist all on the surface of CeO_2.

Fig. 2 shows the TEM images of the catalysts. Fig. 2(a) and (d) clearly show the presence of PdO entity in the PdO/$Ce_{1-x}Pd_xO_{2-\delta}$ and PdO/CeO_2 with a particle size of 3–6 nm, determined by the interplanar distance measurement. On the contrary, no PdO particle was found on the surface of the $Ce_{1-x}Pd_xO_{2-\delta}$ catalyst (Fig. 2(b)), implying that the surface PdO particles in the PdO/$Ce_{1-x}Pd_xO_{2-\delta}$ catalyst could be removed by nitric acid. Note that PdO particle with a particle size of 4 nm × 3 nm was found on the surface of the $Ce_{1-x}Pd_xO_{2-\delta}$-C catalyst in Fig. 2(c). This confirms that some Pd species in the crystal of the $Ce_{1-x}Pd_xO_{2-\delta}$ solid solution migrate to the surface to form surface PdO species, which is consistent with the analysis of the XRD results.

3.2. Surface oxidation state of Pd species in the catalysts

Fig. 3 shows the Pd 3d XPS spectra of the catalysts. For the PdO/$Ce_{1-x}Pd_xO_{2-\delta}$ catalyst, four peaks at 336.8, 337.9, 342.2 and 343.3 eV could be found. The peaks at 336.8 and 342.2 eV could be assigned to PdO [20,21], while those at 337.9 and 343.3 eV could be attributed to PdO_2 [22]. After the nitric acid treatment (the $Ce_{1-x}Pd_xO_{2-\delta}$ catalyst), the peaks attributed to PdO disappear and those assigned to PdO_2 still remain, but with much weaker intensity compared to those of the PdO/$Ce_{1-x}Pd_xO_{2-\delta}$ catalyst. For the $Ce_{1-x}Pd_xO_{2-\delta}$-C catalyst, the peaks characteristic of PdO re-emerge but their intensities are weaker than those of the PdO/$Ce_{1-x}Pd_xO_{2-\delta}$ catalyst. These results are consistent with the previous findings [11], that is, the chemical states of Pd species are mainly Pd^{2+} and Pd^{4+} in the PdO/$Ce_{1-x}Pd_xO_{2-\delta}$ catalyst, Pd^{4+} in the $Ce_{1-x}Pd_xO_{2-\delta}$ catalyst and Pd^{2+} and Pd^{4+} in the $Ce_{1-x}Pd_xO_{2-\delta}$-C catalyst. Also, note that the peak intensity of the Pd^{4+} species is much weaker in the $Ce_{1-x}Pd_xO_{2-\delta}$ catalyst than that in the PdO/$Ce_{1-x}Pd_xO_{2-\delta}$ catalyst and the surface PdO_x species in the PdO/$Ce_{1-x}Pd_xO_{2-\delta}$ catalyst were removed after the acid treatment, it implies that the surface PdO_x species contain a mixture of Pd^{2+} and Pd^{4+} cations and therefore $x = 1–2$.

Furthermore, surface atomic ratio of Pd/Ce for all the catalysts are calculated and listed in Fig. 3. For the PdO/$Ce_{1-x}Pd_xO_{2-\delta}$ catalyst, the Pd/Ce ratio is 0.12, but after acid treatment, this value declines to 0.03 for the $Ce_{1-x}Pd_xO_{2-\delta}$ catalyst, indicating that majority of the surface Pd species is removed after the acid treatment. When calcined at 500 °C in air for 4 h, the Pd/Ce ratio is 0.04 for the $Ce_{1-x}Pd_xO_{2-\delta}$-C catalyst, which is slightly higher than that of the $Ce_{1-x}Pd_xO_{2-\delta}$ catalyst (0.03). This implies an enrichment of the Pd species on the surface after calcinations, which probably due to the migration of Pd^{4+} species from the $Ce_{1-x}Pd_xO_{2-\delta}$ solid solution to the surface. These results agree well with the XRD (Table 1) and HRTEM (Fig. 2) results, confirming the presence of PdO_x ($x = 1–2$) species on the catalyst surface and Pd^{4+} species in the $Ce_{1-x}Pd_xO_{2-\delta}$ solid solution.

3.3. DRIFT spectra of CO chemisorption on the catalysts

Fig. 4 shows the DRIFT spectra of CO chemisorption over the catalysts. It can be seen that there are three strong adsorption peaks for the PdO/$Ce_{1-x}Pd_xO_{2-\delta}$ and PdO/CeO_2 catalysts, with the intensities much stronger for the PdO/$Ce_{1-x}Pd_xO_{2-\delta}$ compared to those for the PdO/CeO_2. The band at 2085 or 2094 cm^{-1} is assigned to the linear adsorption of CO on metallic Pd, and the bands in region of 1900–2000 cm^{-1} are assigned to the isolated bridged and

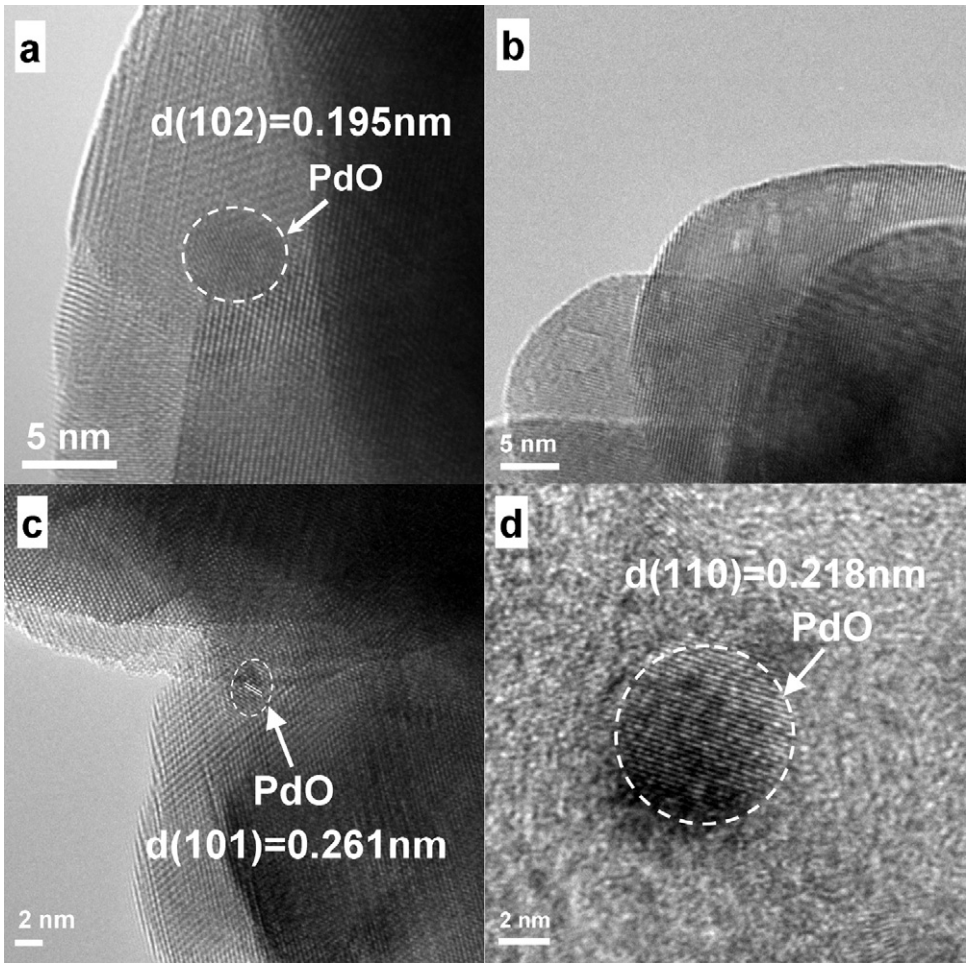

Fig. 2. TEM images of (a) PdO/$Ce_{1-x}Pd_xO_{2-\delta}$, (b) $Ce_{1-x}Pd_xO_{2-\delta}$, (c) $Ce_{1-x}Pd_xO_{2-\delta}$-C, (d) PdO/CeO_2 catalysts.

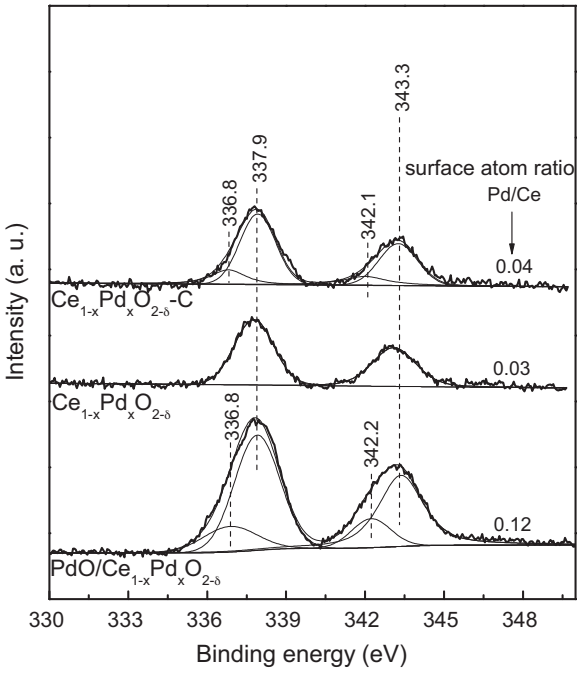

Fig. 3. DRIFT spectra of CO chemisorption over the PdO/CeO_2, PdO/$Ce_{1-x}Pd_xO_{2-\delta}$, $Ce_{1-x}Pd_xO_{2-\delta}$ and $Ce_{1-x}Pd_xO_{2-\delta}$-C catalysts.

compressed bridged adsorption of CO on metallic Pd [23]. There are no bands at ranges of 2120–2110 and 2180–2160 cm^{-1} attribute to CO adsorbed on Pd^+ and Pd^{2+} ions, suggesting that the surface PdO could be readily reduced by CO at ambient conditions [24]. For the $Ce_{1-x}Pd_xO_{2-\delta}$ catalyst, no obvious bands are also observed in the region of 1800–2400 cm^{-1}, indicating that CO molecules can hardly chemisorb on the surface of $Ce_{1-x}Pd_xO_{2-\delta}$ solid solution under experiment conditions. However, for the $Ce_{1-x}Pd_xO_{2-\delta}$-C catalyst, there is a weak band at 2088 cm^{-1}, which is also assigned to the linear adsorption of CO on metallic Pd. This indicates that there are PdO_x species on the surface of $Ce_{1-x}Pd_xO_{2-\delta}$-C catalyst, which is in accordance with the XRD, HRTEM and XPS results. Moreover, the intensity of the 2088 cm^{-1} band is much weaker than that of the PdO/$Ce_{1-x}Pd_xO_{2-\delta}$ catalyst, suggesting that the content of the surface PdO_x species migrated from lattice is much lower than 0.2 wt.%.

3.4. Catalytic activity

Fig. 5 shows the catalytic activities of PdO/$Ce_{1-x}Pd_xO_{2-\delta}$, $Ce_{1-x}Pd_xO_{2-\delta}$, $Ce_{1-x}Pd_xO_{2-\delta}$-C and PdO/CeO_2 catalysts for CO and CH_4 oxidation. For CO oxidation, it can be seen that the PdO/$Ce_{1-x}Pd_xO_{2-\delta}$ catalyst has the highest activity with a complete CO conversion at 140 °C. However, after treating PdO/$Ce_{1-x}Pd_xO_{2-\delta}$ catalyst with nitric acid, the activity of the $Ce_{1-x}Pd_xO_{2-\delta}$ catalyst is dramatically suppressed, with a complete CO conversion at 220 °C. Meanwhile, the $Ce_{1-x}Pd_xO_{2-\delta}$-C catalyst is more active than the $Ce_{1-x}Pd_xO_{2-\delta}$ catalyst. For CH_4 oxidation, the $Ce_{1-x}Pd_xO_{2-\delta}$

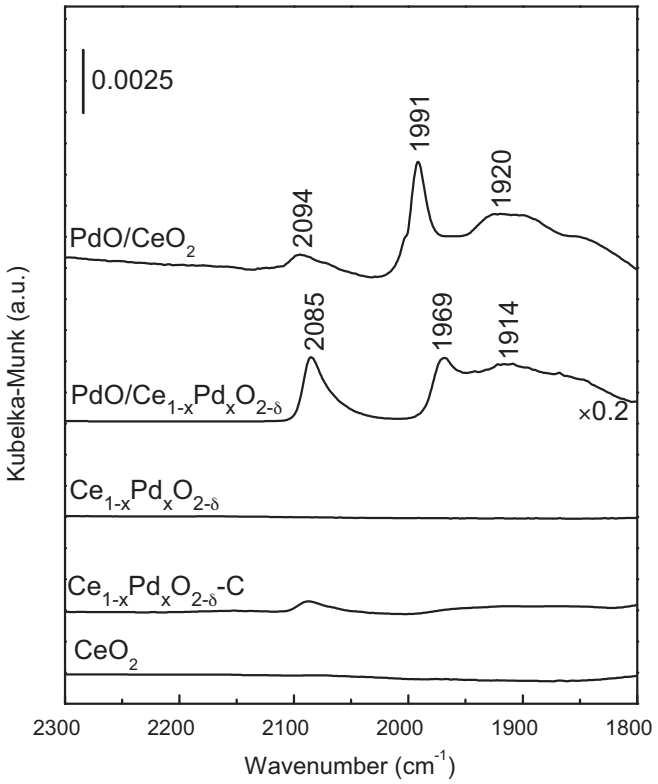

Fig. 4. Pd 3d XPS spectrum of $PdO/Ce_{1-x}Pd_xO_{2-\delta}$, $Ce_{1-x}Pd_xO_{2-\delta}$ and $Ce_{1-x}Pd_xO_{2-\delta}$-C catalysts.

catalyst has the highest activity, and the $Ce_{1-x}Pd_xO_{2-\delta}$-C catalyst has the medium activity, while the $PdO/Ce_{1-x}Pd_xO_{2-\delta}$ catalyst has lower activity than $Ce_{1-x}Pd_xO_{2-\delta}$-C catalyst. It is also found that the PdO/CeO_2 catalyst prepared by the impregnation method is much less active than those prepared by the solution combustion method, but the pure CeO_2 possesses the lowest activity.

According to the data in Fig. 5, specific reaction rate of each catalyst based on Pd content could be calculated, as shown in Table 2. For CO oxidation, concerning the contribution of individual Pd species to the activity, it can be seen that PdO_x species on the surface of $PdO/Ce_{1-x}Pd_xO_{2-\delta}$ and PdO/CeO_2 catalysts have the activity of 673.4 $\mu mol_{CO}\, g_{Pd}^{-1}\, s^{-1}$ and 6.1 $\mu mol_{CO}\, g_{Pd}^{-1}\, s^{-1}$,

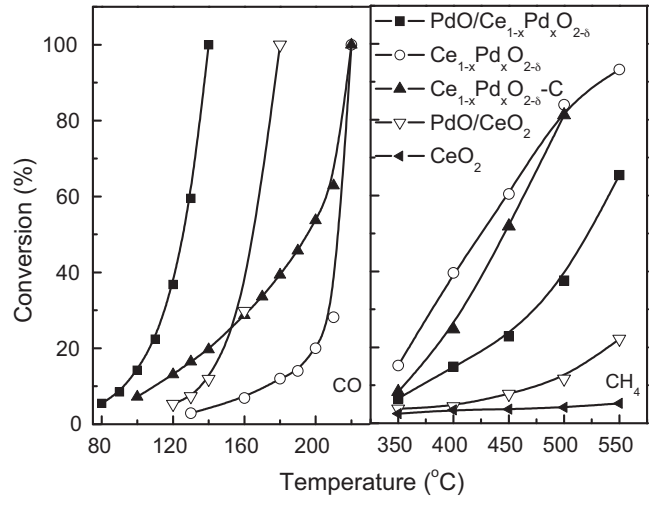

Fig. 5. Catalytic activities of $PdO/Ce_{1-x}Pd_xO_{2-\delta}$, $Ce_{1-x}Pd_xO_{2-\delta}$, PdO/CeO_2 and $Ce_{1-x}Pd_xO_{2-\delta}$-C catalysts for CO and CH_4 oxidation.

which are much higher than Pd^{4+} species in $Ce_{1-x}Pd_xO_{2-\delta}$ (2.7 $\mu mol_{CO}\, g_{Pd}^{-1}\, s^{-1}$), indicating that surface PdO_x species favor CO oxidation. For the $Ce_{1-x}Pd_xO_{2-\delta}$-C catalyst, the specific reaction rate (15.6 $\mu mol_{CO}\, g_{Pd}^{-1}\, s^{-1}$) is higher than that of the $Ce_{1-x}Pd_xO_{2-\delta}$ catalyst (2.7 $\mu mol_{CO}\, g_{Pd}^{-1}\, s^{-1}$), again confirming the promoting effect of surface PdO_x species for CO oxidation, because Pd^{4+} cations migrate from the CeO_2 lattice and form surface PdO_x entities, as evidenced by XRD (Table 1), TEM (Fig. 2), XPS (Fig. 3) and DRIFTS (Fig. 4) results. The higher activity of surface PdO_x species is due to the fact that these species provide CO chemisorption sites (Fig. 4), which makes the CO activation much easier compared to the Pd^{4+} species in the $Ce_{1-x}Pd_xO_{2-\delta}$ solid solution. Meanwhile, the higher reactivity of the PdO_x species on the surface of the $PdO/Ce_{1-x}Pd_xO_{2-\delta}$ (673.4 $\mu mol_{CO}\, g_{Pd}^{-1}\, s^{-1}$) compared to that of the PdO/CeO_2 catalyst (6.1 $\mu mol_{CO}\, g_{Pd}^{-1}\, s^{-1}$) could be interpreted by synergetic effects of PdO_x species on the surface and in the CeO_2 lattice, with the $Ce_{1-x}Pd_xO_{2-\delta}$ solid solution generating higher oxygen vacancy concentration than pure CeO_2. For example, in our previous work, it was found that a similar $PdO/Ce_{1-x}Pd_xO_{2-\delta}$ prepared using the solution-combustion method contains a relative oxygen vacancy concentration of 1.6, which is much higher than that of a PdO/CeO_2 (1.0) prepared using the impregnation method due to the formation of $Ce_{1-x}Pd_xO_{2-\delta}$ solid solution [17]. Such synergetic effects could also explain the higher reactivity of the $Ce_{1-x}Pd_xO_{2-\delta}$-C catalyst compared to that of the PdO/CeO_2 catalyst. Interestingly, Priolkar et al. [11] also compared CO oxidation over a Pd/CeO_2 catalyst prepared by the solution-combustion method and a similar catalyst prepared by the impregnation method, and concluded that the Pd species in the CeO_2 lattice are more active than the surface PdO_x species. This is inconsistent with the findings in the current work, which lies in the fact that the Pd/CeO_2 catalyst prepared by the solution-combustion method still contained very limited surface PdO_x species, as evidenced in our previous work [17].

For CH_4 oxidation, the situation is quite different. As the specific reaction rate of the $Ce_{1-x}Pd_xO_{2-\delta}$ catalyst (7.5 $\mu mol_{CH_4}\, g_{Pd}^{-1}\, s^{-1}$) is larger than those of the $PdO/Ce_{1-x}Pd_xO_{2-\delta}$ (2.8 $\mu mol_{CH_4}\, g_{Pd}^{-1}\, s^{-1}$) and the PdO/CeO_2 (1.7 $\mu mol_{CH_4}\, g_{Pd}^{-1}\, s^{-1}$) catalysts, implying that the surface PdO_x species are less active than the Pd^{4+} in the $Ce_{1-x}Pd_xO_{2-\delta}$ solid solution and the latter contributes more to the reaction than the surface PdO_x species. Although detection of reaction intermediates evolution for CH_4 oxidation over these catalysts at reaction conditions could be highly desirable like in the case of CO oxidation (Fig. 4), investigation of CH_4 chemisorption by DRIFT are not successful at 350 °C. No relevant intermediates are found except carbonate residues. Nevertheless, our results are consistent with the findings reported by Colussi et al. [16] that the nanofaceted Pd–O sites in Pd–Ce surface structures contributed high activity in catalytic combustion of CH_4. Also, the enhanced activity of Pd–O–Ce entities in $Ce_{1-x}Pd_xO_{2-\delta}$ has been confirmed by theoretical calculation. For example, Mayernick et al. [15,18] found that the methane activation barrier over the $Ce_{1-x}Pd_xO_{2-\delta}$ (1 1 1) surface is lower than that over PdO (1 0 0), and CeO_2 (1 1 1), (1 1 0), (1 0 0) surfaces, which is due to the enhanced reducibility of CeO_2 surface by the incorporation of Pd ions into the CeO_2 lattice. Moreover, the enhanced activity of $Ce_{1-x}Pd_xO_{2-\delta}$ solid solution is also evidenced by the reaction rate of the $Ce_{1-x}Pd_xO_{2-\delta}$-C catalyst with very limited amount of PdO_x species (Pd content is less than 0.2 wt.%) on the $Ce_{1-x}Pd_xO_{2-\delta}$ solid solution surface, which has lower activity than pure $Ce_{1-x}Pd_xO_{2-\delta}$ solid solution. It is again reveals that $Ce_{1-x}Pd_xO_{2-\delta}$ species are more active than the surface PdO_x. The suppressed activity by surface PdO_x species may be due to the coverage of PdO_x entities on the surface of $Ce_{1-x}Pd_xO_{2-\delta}$ solid solution, which decreases the amount of active sites and consequently causes a decline in the activity. This may also explain the unstable $PdO–CeO_2$ catalysts for CH_4 oxidation, resulting from the migration

Table 2
Specific reaction rates of different catalysts for CO and CH_4 oxidation.

Catalyst	Pd content (wt.%)		Conv. (%)		Specific reaction rate ($\mu mol\ g_{Pd}^{-1}\ s^{-1}$)			
					CO		CH_4	
	Total	Surface PdO_x	CO[c]	CH_4[d]	Total	Surface PdO_x	Total	Pd^{4+} in $Ce_{1-x}Pd_xO_{2-\delta}$
$PdO/Ce_{1-x}Pd_xO_{2-\delta}$	1.70	0.20	9.8[a]	6.5[b]	81.6	673.4	2.8	–
$Ce_{1-x}Pd_xO_{2-\delta}$[b]	1.50	–	2.9	15.2	2.7	–	7.5	7.5
$Ce_{1-x}Pd_xO_{2-\delta}$-C[b]	1.50	–	16.5	8.3	15.6	–	4.1	–
PdO/CeO_2[b]	1.68	1.68	7.3	3.9	6.1	6.1	1.7	–

[a] The catalyst weight is 20 mg, homogeneously mixed with 180 mg quartz sand with same meshes.
[b] The catalyst weight is 200 mg.
[c] Reaction temperature = 130 °C.
[d] Reaction temperature = 350 °C.

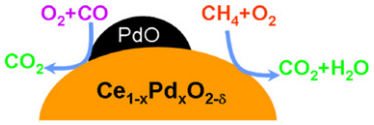

Scheme 1. Reaction models of CO and CH_4 oxidation over $PdO–CeO_2$ catalyst.

of active Pd^{4+} ions from CeO_2 lattice to surface during high temperature reaction. However, variation in the reaction pathway due to the structural change of the catalyst could not be excluded and needs a further investigation.

Therefore, it can be seen that different active sites are required for CO and CH_4 oxidation reactions. The surface PdO_x species favor CO oxidation reaction, while the $Ce_{1-x}Pd_xO_{2-\delta}$ solid solution favors CH_4 oxidation. Scheme 1 shows the reaction models of CO and CH_4 oxidation over the catalyst. However, even though the roles of different Pd species in CO and CH_4 oxidation could be clearly distinguished as shown in this work, one must realize that they are not 100% conclusive because of the complexity of the catalyst system. The $PdO/Ce_{1-x}Pd_xO_{2-\delta}$ catalyst employed in the current work contains a heterogeneous set of possible active sites differing in PdO_x particle size/structure, solid solution crystallite size, surface termination of the oxide, and so on, which would consequently influence the reactivity of the catalyst.

4. Conclusion

This work demonstrates the different roles of Pd species in CO and CH_4 oxidation, as well as the quantitative analysis of their contributions in these two reactions. The surface PdO_x species in the $PdO/Ce_{1-x}Pd_xO_{2-\delta}$ catalyst can be removed by nitric acid treatment, while Pd^{4+} species in the $Ce_{1-x}Pd_xO_{2-\delta}$ solid solution remain intact. The surface PdO_x species are very active for CO oxidation, while the Pd^{4+} species in the $Ce_{1-x}Pd_xO_{2-\delta}$ solid solution are active for CH_4 oxidation. Also, transformation of Pd species is detected, namely, Pd^{4+} ions in CeO_2 lattice could migrate to surface at high temperature and form PdO_x species.

Acknowledgment

This work was financially supported by Natural Science Foundation of China (Grant No. 21173195).

References

[1] P. Glin, M. Primet, Appl. Catal. B 39 (2002) 1–37.
[2] W.S. Epling, G.B. Hoflund, J. Catal. 182 (1999) 5–12.
[3] G. Zhou, P.R. Shah, T. Montini, P. Fornasiero, R.J. Gorte, Surf. Sci. 601 (2007) 2512–2519.
[4] B. Wang, D. Weng, X.D. Wu, J. Fan, Catal. Today 153 (2010) 111–117.
[5] P. Gélin, M. Primet, Appl. Catal. B 39 (2002) 1–37.
[6] W.Y. Hernández, F. Romero-Sarria, M.A. Centeno, J.A. Odriozola, J. Phys. Chem. C 114 (2010) 10857–10865.
[7] X. Wang, R.J. Gorte, J.P. Wagner, J. Catal. 212 (2002) 225–230.
[8] Y. Matsumura, W.J. Shen, Y. Ichihashi, H. Ando, Catal. Lett. 68 (2000) 181–183.
[9] L.H. Xiao, K.P. Sun, X.L. Xu, X.N. Li, Catal. Commun. 6 (2005) 796–801.
[10] H.W. Jen, G.W. Graham, W. Chun, R.W. McCabe, J.P. Cuif, S.E. Deutsch, O. Touret, Catal. Today 50 (1999) 309–328.
[11] K.R. Priolkar, P. Bera, P.R. Sarode, M.S. Hegde, S. Emura, R. Kumashiro, N.P. Lalla, Chem. Mater. 14 (2002) 2120–2128.
[12] R.F. Hicks, H.H. Qi, M.L. Young, R.G. Lee, J. Catal. 122 (1990) 280–294.
[13] M.F. Luo, Z.Y. Pu, M. He, J. Jin, L.Y. Jin, J. Mol. Catal. A: Chem. 260 (2006) 152–156.
[14] S.H. Oh, G.B. Hoflund, J. Phys. Chem. A 110 (2006) 7609–7613.
[15] A.D. Mayernick, M.J. Janik, J. Catal. 278 (2010) 16–25.
[16] S. Colussi, A. Gayen, M.F. Camellone, M. Boaro, J. Llorca, S. Fabris, A. Trovarelli, Angew. Chem. Int. Ed. 48 (2009) 8481–8484.
[17] L. Meng, A.P. Jia, J.Q. Lu, L.F. Luo, W.X. Huang, M.F. Luo, J. Phys. Chem. C 115 (2011) 19789–19796.
[18] A.D. Mayernick, M.J. Janik, J. Phys. Chem. C 112 (2008) 14955–14964.
[19] M.S. Hegde, G. Madras, K.C. Patil, Acc. Chem. Res. 42 (2009) 704–712.
[20] T. Pillo, R. Zimmermann, P. Steiner, S. Hüfner, J. Phys. Condens. Matter 9 (1997) 3987–3999.
[21] M. Burn, A. Berthet, J.C. Bertolini, J. Electron Spectrosc. Relat. Phenom. 104 (1999) 55–60.
[22] Z.J. Zuo, W. Huang, P.D. Han, Z.H. Li, J. Mol. Struct. 936 (2009) 118–124.
[23] A. Bensalem, J.C. Muller, D. Tessier, F. Bozon-Verduraz, J. Chem. Soc., Faraday Trans. 92 (1996) 3233–3237.
[24] D. Tessier, A. Rakai, F. Bozon-Verduraz, J. Chem. Soc., Faraday Trans. 88 (1992) 741–749.